Human Molecular Genetics, 2003, Vol. 12, No. 4 **379–388**
DOI: 10.1093/hmg/ddg032

Clinical and functional effects of a deletion in a COOH-terminal lumenal loop of the skeletal muscle ryanodine receptor

Francesco Zorzato[1,2], Naohiro Yamaguchi[3], Le Xu[3], Gerhard Meissner[3], Clemens R. Müller[4], Pierre Pouliquin[2], Francesco Muntoni[5], Caroline Sewry[5], Thierry Girard[1] and Susan Treves[1,*]

[1]Departments für Anaesthesie und Forschung, Kantonsspital Basel, 4031 Basel, Switzerland, [2]Dipartimento di Medicina Sperimentale e Diagnostica, Università di Ferrara, 44100 Ferrara, Italy, [3]Departments of Biochemistry and Biophysics and Molecular and Cellular Physiology, University of North Carolina, Chapel Hill, NC 27599-7260, USA, [4]Institut für Humangenetik, Biozentrum der Universität Würzburg, 97074 Würzburg, Germany and [5]The Dubowitz Neuromuscular Centre, Imperial College School of Medicine, London W12 0NN, UK

Received October 25, 2002; Revised and Accepted December 3, 2002

We have identified a patient affected by a relatively severe form of central core disease (CCD), carrying a heterozygous deletion (amino acids 4863–4869) in the pore-forming region of the sarcoplasmic reticulum calcium release channel. The functional effect of this deletion was investigated (i) in lymphoblastoid cells from the affected patient and her mother, who was also found to harbour the mutation and (ii) in HEK293 cells expressing recombinant mutant channels. Lymphoblastoid cells carrying the RYR1 deletion exhibit an 'unprompted' calcium release from intracellular stores, resulting in significantly smaller thapsigargin-sensitive intracellular Ca^{2+} stores, compared with lymphoblastoid cells from control individuals. Blocking the RYR1 with dantrolene restored the intracellular calcium stores to levels similar to those found in control cells. Single channel and [^{3}H]ryanodine binding measurements of heterologously expressed mutant channels revealed a reduced ion conductance and loss of ryanodine binding and regulation by Ca^{2+}. Heterologous expression of recombinant RYR1 peptides and analysis of their membrane topology demonstrate that the deleted amino acids are localized in the lumenal loop connecting membrane-spanning segments M8 and M10. We provide evidence that a deletion in the lumenal loop of RYR1alters channel function and causes CCD.

INTRODUCTION

The ryanodine receptors (RYR) are a family of intracellular calcium release channels found in a variety of tissues and cell types. At least three different isoforms have been identified and characterized at the molecular level (for review see 1). Type 1 RYR is predominantly expressed in skeletal muscle and is encoded by a gene of 106 exons that maps to human chromosome 19q13.1 (2). The human RYR1 gene encodes 5037 amino acids giving rise to one of the largest known proteins (3,4). The functional calcium release channel assembles as a macromolecular complex of more than 2.5 MDa and is composed of four RYR1 subunits of 565 kDa each and a number of accessory proteins which are thought to regulate and stabilize the calcium channel (5–7).

To date more than 40 missense mutations have been identified in the RYR1 gene and are associated with central core disease (CCD; OMIM no.117000) and/or the malignant hyperthermia susceptible phenotype (MHS; OMIM no.145600) (for recent reviews see 8–10). CCD is a rare congenital myopathy of autosomal dominant inheritance (11,12). Affected individuals present with infantile hypotonia (floppy infant syndrome) and a delay in achieving motor milestones. Later in life, the predominant symptom is a generalized muscle weakness affecting the proximal muscle groups more than the distal ones. The clinical severity is highly variable, but the course is usually slow or non-progressive. Additional clinical features may include congenital hip dislocation, kyphoscoliosis, foot deformities and joint contractures. The diagnosis is

*To whom correspondence should be addressed at: ZLF Basel Kantonsspital, Lab 408, Hebelstrasse 20, 4031 Basel, Switzerland. Tel: +41 612652373; Fax: +41 612653702; Email: susan.treves@unibas.ch

difficult on the basis of clinical findings alone and a histological examination of muscle tissue is essential. Typically, type I fibres predominate and, on cross sections, contain single, well-demarcated and centrally located cores, which do not stain with oxidative and phosphorylase histochemical stains. In longitudinal sections the amorphous-looking areas run along the length of the fibres (13–15).

Malignant hyperthermia (MH) is an autosomal dominant pharmacogenetic disease triggered by volatile anaesthetics and depolarizing muscle relaxants in genetically predisposed individuals (16–18). Symptoms include skeletal muscle rigidity, tachycardia, hyperthermia, acidosis, cardiac arrhythmias and rhabdomyolysis (8,19,20). In some individuals MH reactions appear to be triggered by physical exercise and emotional stress, leading some authors to suggest that MH, heat stroke and exercise-induced rhabdomyolysis have a common denominator (18,21,22).

The mutated codons giving rise to CCD and MH are clustered in three regions of the RYR1 gene: region 1, extending from Met1 to Arg614; region 2, extending between Arg2162 and Arg2458; and region 3, which spans the highly conserved C-terminal domain encompassing amino acid sequences which are predicted to form the membrane spanning segment of the calcium release channel. The majority of RYR1 mutations giving rise to MH and CCD were found in regions 1 and 2; recently however, 16 novel mutations predominantly associated with CCD were found in exons 94–106 (23–25).

Although RYR1 was thought to be almost exclusively expressed in skeletal muscle, several reports have demonstrated that circulating human B-lymphocytes, Epstein–Barr Virus (EBV)-immortalized lymphoblastoid cells and murine dendritic cells express a functional type 1 RYR calcium release channel (24,26–28). Thus, measurements of the intracellular Ca^{2+} concentration, $[Ca^{2+}]_i$ in EBV-immortalized lymphoblastoid cells from patients can be used to assay the function of RYR1 mutations *ex vivo* (24,26). In the present study we characterized the functional properties of RYR1s carrying a deletion which was identified in a patient with a severe form of CCD.

RESULTS

RYR1 mutation analysis

Upon mutation screening by SSCA an aberrant fragment was noted in exon 101 of the patient's DNA. Subsequent sequencing disclosed a deletion of nucleotides 14588–14606 (TCTACAACAAGAGCGAGG) in the heterozygous state. The deletion was also present in the DNA of the patient's mildly affected mother but absent in her healthy father. Figure 1 shows an agarose gel of the PCR amplified DNA products: the genomic DNA from the unaffected father exhibited a 176 bp DNA fragment while amplification of the DNA from the proband and her mother yielded two fragments of 176 bp (wild-type) and 158 bp (deletion). The deletion results in the removal of seven amino acids (4863–4869, FYNKSED) and insertion of a novel tyrosine residue (RYR1 Δ4863–4869 deletion mutant), thus leading to a net in-frame deletion of six amino acids. Figure 2 shows that the deleted amino acids are present and conserved in all known vertebrate RYR isoforms.

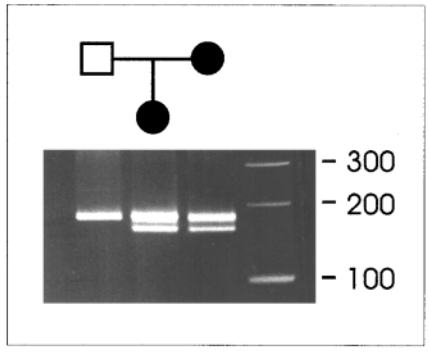

RYR1, exon 101, wildtype

N F F R K **F Y N K S E** D E D E P D M K C D

AACTTCTTCCGCAAGT**TCTACAACAAGAGCGAGG**ATGAGGATGAACCTGACATGAAGTGTGAT

RYR1, exon 101, deletion

N F F R K Y E D E P D M K C D

AACTTCTTCCGCAAGTATGAGGATGAACCTGACATGAAGTGTGAT

Figure 1. Identification of a RYR1 deletion in a patient affected by severe CCD and in her mildly affected mother. Genomic DNA was amplified by PCR using a set of primers spanning exon 101 of the RYR1 gene; DNA fragments were separated on a 3% agarose gel. Amplification of the unaffected father's DNA yielded a single band of 176 bp, while amplification of the affected daughter's and mother's DNA yielded two bands of 176 and 158 bp, respectively, indicating a deletion of 18 bp in one allele.

Functional studies of cells expressing the native mutated RYR1 calcium channel

We used EBV-immortalized lymphoblastoid cells from the proband and her mother to study the functional effect of the newly identified RYR1 Δ4863–4869 deletion mutant. The presence of the RYR1 gene mutation in the cell lines was checked by PCR amplification using a set of primers spanning exons 100–101. As shown in Figure 3A the cDNA prepared from EBV-immortalized lymphoblastoid cells from the proband showed two bands of 224 and 206 bp, while the cDNA prepared from control lymphoblastoid cells showed one band of 224 bp. The identity of the cDNA fragment was confirmed by direct sequencing (not shown).

We proceeded to test the functional effect of the RYR1 deletion on intracellular calcium homeostasis. Lymphoblastoid cells were loaded with the fluorescent calcium indicator fura-2/AM and their $[Ca^{2+}]_i$ monitored in nominally Ca^{2+}-free EGTA-containing Krebs–Ringer buffer. Figure 3B shows that cells harbouring the RYR1 deletion released calcium from intracellular stores when placed in Krebs–Ringer medium containing 0.5 mM EGTA. This increase in fluorescent ratio did not occur in cells from control individuals (Fig. 3C). The released calcium was contained within an intracellular store endowed with a SERCA type Ca-ATPase since the addition of 400 nM thapsigargin failed to cause a further increase in the $[Ca^{2+}]_i$, whereas the addition of thapsigargin to cells from control individuals caused an immediate transient increase in the $[Ca^{2+}]_i$ (panel 3C). The 'unprompted' calcium release was

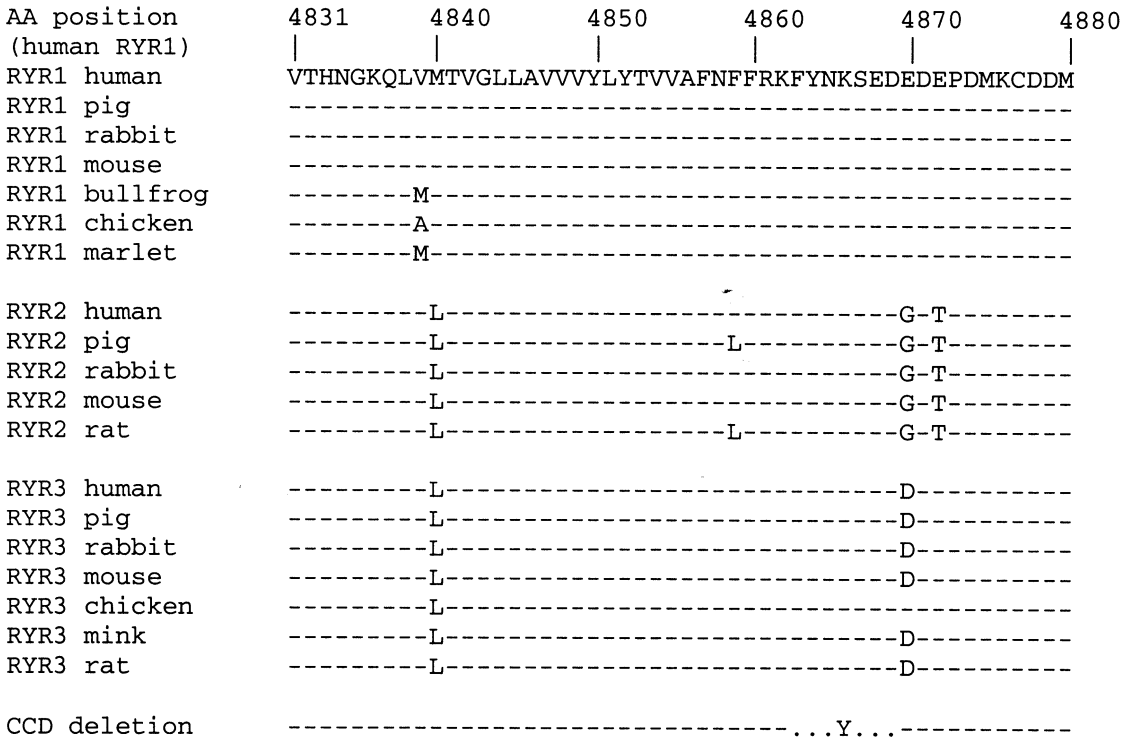

Figure 2. Alignment of the COOH-terminal region encompassing the deleted amino acids in 19 vertebrate RYR genes. Identical amino acids are indicated by a horizontal dash. The last line indicates the deletion found in the present patients.

seen in nine out of 14 experiments. However, in those experiments in which no transient was observed, the thapsigargin-sensitive intracellular stores were smaller than those observed in cells from control individuals. The results depicted in Figure 3D show that the presence of the RYR1 Δ4863–4869 deletion causes a significant depletion of calcium from the thapsigargin sensitive stores ($*P < 0.0001$). In order to confirm that the calcium release was due to a leaky RYR1 channel, we carried out experiments in the presence of dantrolene, a specific inhibitor of the skeletal muscle ryanodine receptor (29,30). Pre-treatment of cells with 10 μM dantrolene blocked the 'unprompted' calcium release from the cells harbouring the RYR1 Δ4863–4869 deletion (see insert traces in Fig. 3B) and brought the thapsigargin-sensitive $[Ca^{2+}]_i$ stores of the cell lines harbouring the RYR1 Δ4863–4869 deletion, to levels indistinguishable from those of controls (Fig. 3D; $P > 0.5$).

Functional properties of cells transiently expressing the recombinant RYR1 Δ4863–4869 deletion mutant

In order to directly study the biophysical properties of RYR1 carrying the homozygously expressed deletion, we constructed the full-length rabbit RYR1 cDNA carrying a deletion of amino acids 4863–4869 and transiently expressed it in HEK293 cells. Under our experimental conditions, cells transfected with this construct showed no noticeable activity, as determined by [^{3}H]ryanodine binding [0.15 ± 0.05 and <0.02 pmol/mg protein for wild-type (wt)-RYR1 and RYR1 Δ4863–4869, respectively, $n = 3$]. The absence of binding was not due to lack of expression of the deleted protein, as a major immunoreactive band with an intensity comparable to wt-RYR1 was visible on western blots (Fig. 4A). The presence of an ion conducting activity in the RYR1 Δ4863–4869 deletion mutant was determined in single-channel measurements with the planar lipid bilayer method. Channels carrying the deletion were less stable than the wild-type channels and disappeared rapidly when recorded at membrane potentials greater than ± 20 mV. As shown in Fig. 4B, a decrease in *cis* (cytosolic) Ca^{2+} concentration from 2 μM to 130 nM nearly fully closed the wild-type channel. In contrast, mutant channel activity was not noticeably affected when the *cis* Ca^{2+} concentration was lowered from 2 μM to 130 nM (Fig. 4B) or to 1 nM (not shown). The mutant channels were not modified by ryanodine and their K^+ conductance was lower than that of the wild-type recombinant RYR1 (conductance of ∼576 pS, which is lower than that of the wild-type recombinant RYR1 of ∼785 pS; Fig. 4B and D). Wild-type and mutant channels were identified by their ability to conduct Ca^{2+} (2.2 and 0.8 pA for wild-type and mutant channels, respectively, at 0 mV with 10 mM Ca^{2+} as current carrier; Fig. 4C) and their inhibition by ruthenium red (Fig. 4C), a potent inhibitor of the RyRs (31).

Membrane topology of the domain encompassing RYR1 Δ4863–4869 deletion

In order to determine the topology of the portion of the RYR encompassing the deleted amino acids, we cloned the rabbit RYR1 cDNA sequences encompassing putative domain M8 (amino acids V4830 to D4870, corresponding to a peptide with a calculated molecular mass of 4945 Da) and M10 (amino acids

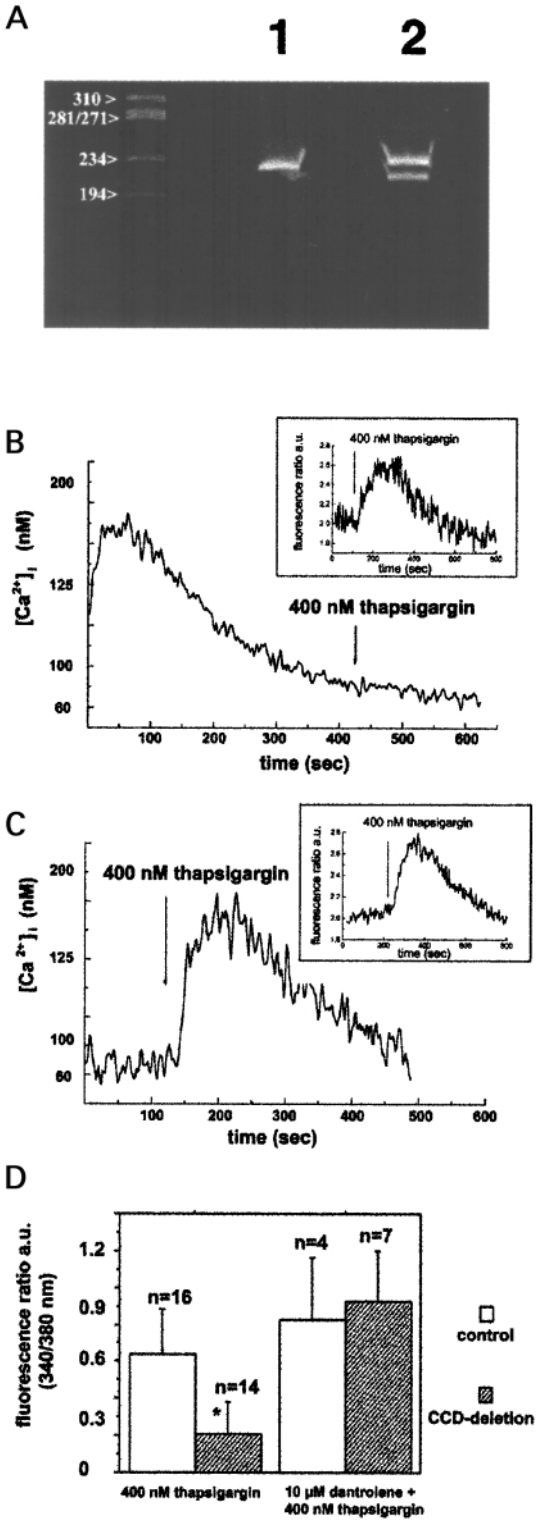

Figure 3. EBV-immortalized lymphoblastoid cells from the patient harbouring the RYR1 Δ4863–4869 deletion mutant release calcium in the absence of RYR activators. (**A**) 7.5% polyacrylamide gel showing that PCR amplification of cDNA from lymphoblastoid cells with primers spanning exons 100–101 of the human RYR1 gene gives rise to a band of 224 bp (lane 1, DNA from control cells) or a doublet of 224 and 206 bp (lane 2, DNA amplification from the proband carrying the RYR1 Δ4863–4869 deletion mutant. (**B** and **C**) Cells were loaded with the fluorescent calcium indicator fura-2/AM as described in the Methods section. Prior to the $[Ca^{2+}]_i$ measurements, 0.75×10^6 cells/ml were centrifuged, resuspended in nominally Ca^{2+}-free Krebs–Ringer and placed in the fluorimeter cuvette. Lymphoblastoid cells from the proband carrying the RYR1 Δ4863–4869 deletion mutant exhibit an increase in the $[Ca^{2+}]_i$ in the absence of exogenous trigger agents. The addition of 400 nM thapsigargin caused no further changes in the $[Ca^{2+}]_i$ (B). Lymphoblastoid cells from a control individual did not exhibit the 'unprompted' calcium release and the addition of 400 nM thapsigargin caused an increase in the $[Ca^{2+}]_i$ (C). Traces are representative of experiments carried out at least four times on three different days. The insert of (B) shows that addition of 10 µM dantrolene to the Ca^{2+}-free Krebs–Ringer in the cuvette blocked the unprompted $[Ca^{2+}]_i$ increase observed in the lymphoblastoid cells carrying the deletion. Inserts of (B) and (C) show a typical trace obtained when cells were pretreated with 10 µM dantrolene. (**D**) Peak Ca^{2+} induced by the addition of 400 nM thapsigargin in cells from the individuals carrying the RYR1 Δ4863–4869 deletion mutant or from controls were pre-treated with or without 10 µM dantrolene. Results are expressed as mean peak calcium released (±SD of *n* experiments). $^*P < 0.0001$ using the Student's *t*-test for paired samples.

D4907 to L4943, corresponding to a peptide with a calculated molecular mass of 4544 Da) (3) in-frame at the COOH-terminus of the reporter protein GFP. Tsa201 and COS-7 cells were transfected with the EGFP or the GFP-tagged constructs and membrane fractions prepared. Figure 5A and B shows that the GFP immunoreactivity remained within the integral membrane fraction (P) when the GM8 and GM10 constructs were examined, and no immunoreactivity was present in the soluble fraction (S) after high salt and 100 mM Na_2CO_3 extraction. On the other hand, when cells were transfected with the pEGFP plasmid, the immunoreactive band was in the soluble, post-microsomal supernatant (Fig. 5C). The panels on the right show the GFP fluorescence of COS-7 cells transfected with the three constructs: a diffuse punctuated perinuclear fluorescence, typical of intracellular membrane distribution was obtained upon transfection with GM8 and GM10; this is different from the fluorescence exhibited by cells transfected with the pEGFP plasmid.

To demonstrate that polypeptides M8 and M10 span the membrane when expressed as recombinant proteins in heterologous cells, we also used a sandwich assay: the COOH-termini of both constructs were tagged with a FLAG-tag while the GFP tag was maintained at the NH_2 termini (Fig. 6A). We would like to point out that addition of three copies of the negatively charged FLAG epitope causes the polypeptides to migrate more slowly than expected in SDS–PAGE. Figure 6B shows a western blot of the microsomal proteins (or of proteins present in the post microsomal supernatant) of Tsa 201 cells transfected with pEGFP (lane 1), pEGFP-FLAG (lane 2), GM8FLAG (lane 3) and GM10FLAG (lane 4). The FLAG-tagged constructs have a lower than expected mobility.

The microsomal fractions of Tsa201 cells transfected with the GM8FLAG and GM10FLAG constructs were treated with proteinase K. If the GFP immunoreactivity disappears and that of the FLAG tag remains, then the protein must be oriented with GFP facing the cytoplasm; if the immunoreactivity with both antibodies disappears then the polypeptide does not completely span the bilayer. When experiments were performed with the GM8FLAG construct, the GFP tag was

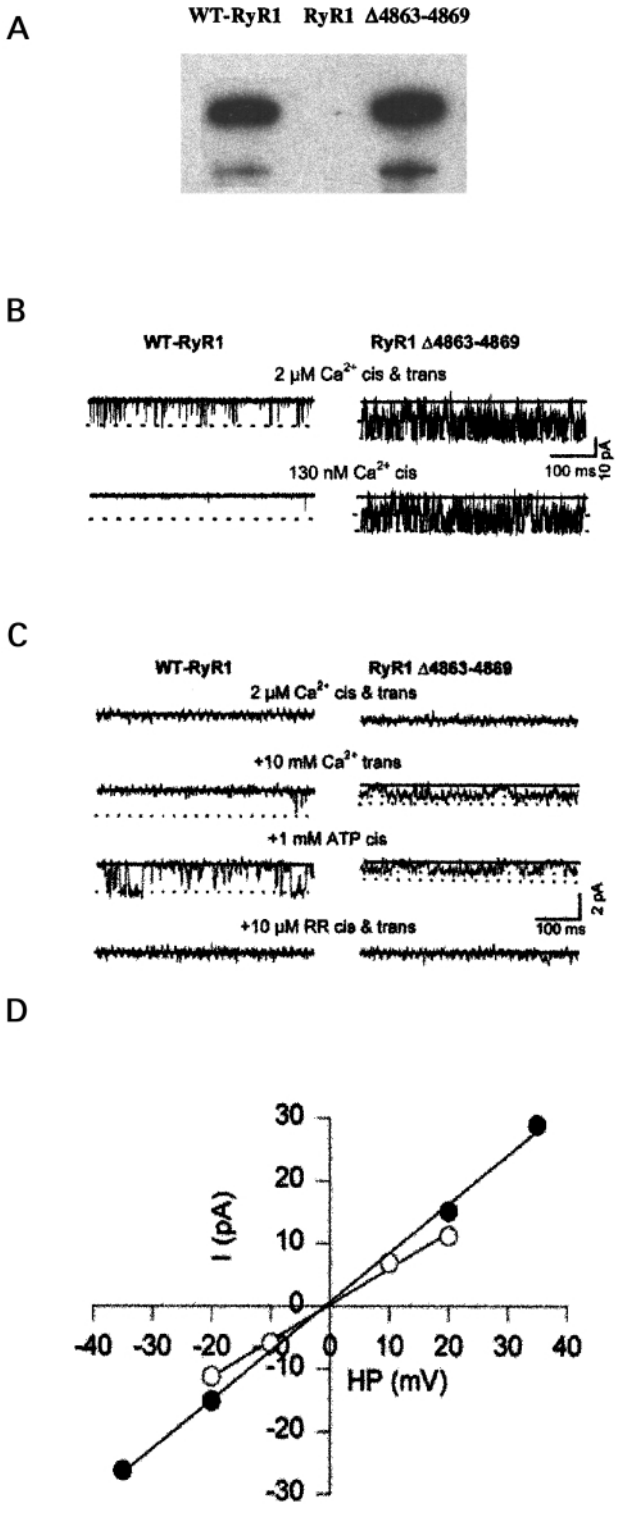

Figure 4. Immunoblots and single channel recordings for wt-RYR1 and RYR1 Δ4863–4869. (**A**) Equal amounts of membranes (6 μg protein/lane) isolated from HEK293 cells expressing wt-RyR1 (left) and RYR1 Δ4863–4869 (right) were probed with a monoclonal antibody raised against RYR1 (mAb D110) as described in Materials and Methods. The upper major bands represent the intact 565 kDa RYR1 peptides and the lower ones proteolysis products. (**B**) One wt-RYR1 (left) and two RYR1 Δ4863–4869 (right) channel currents were recorded at −20 mV in symmetric 250 mM KCl containing the indicated free *cis* Ca^{2+} concentrations and are shown as downward inflections (dotted line, open channel current levels) from a closed state (solid line). Electrical signals were filtered at 2 kHz. Channel open probability (P_o) of wt-RyR1 was 0.12 ± 0.03 and 0.01 ± 0.01 ($n = 16$), and of RYR1 Δ4863–4869 was 0.45 ± 0.08 and 0.43 ± 0.08 ($n = 5$) at 2 μM and 0.13 μM *cis* Ca^{2+}, respectively. (**C**) One wt-RYR1 (left) and two RYR1 Δ4863–4869 (right) channels currents were recorded at 0 mV with 2 μM *cis* and *trans* Ca^{2+} (top traces), after the consecutive addition of 10 mM *trans* Ca^{2+} (second traces), 1 mM *cis* ATP (third traces) and 10 μM *cis* and *trans* ruthenium red (bottom traces). Electrical signals were filtered at 0.3 kHz. Single channel Ca^{2+} currents in traces 2 and 3 were 2.2 ± 0.2 pA ($n = 3$) for wt-RyR1 and 0.8 ± 0.1 pA ($n = 3$) for RYR1 Δ4863–4869). (**D**) Current–voltage relationship of wt (filled circles) and mutant (empty circles) channels in 250 mM symmetric KCl with K^+ as current carrier. Wild-type and mutant channels averaged K^+ conductances were 785 ± 10 pS ($n = 5$) and 576 ± 16 pS ($n = 14$), respectively.

accessible to proteinase K (Fig. 6C); on the other hand the FLAG tag was not accessible to proteinase K and an anti-FLAG immunopositive band of approximately 18 kDa (asterisk in Fig. 6C) was present in the protein extracts after digestion. When the same experimental approach was applied to the GM10FLAG construct, the results were different. In fact, digestion with proteinase K did not eliminate immunoreactivity of the GFP tag, although the immunoreactive band was smaller, confirming proteolysis (Fig. 6D). On the other hand, immunoreactivity of the FLAG tag disappeared after digestion, indicating it faces the cytoplasm.

DISCUSSION

In the present study we identified a patient of European origin affected by CCD, carrying a heterozygous deletion of seven amino acids (and insertion of a Tyr) in the COOH-terminal domain of the RYR1 gene. Most known nucleotide substitutions in the RYR1 associated with MH and CCD replace single amino acids, the most common being the loss or gain of a positively charged arginine residue. Recently Monnier *et al.* (23) reported short (1–3 amino acid) deletions within the COOH-terminal domain of the RYR of patients affected by 'classical' CCD.

In this study we extended previous results (24,26) by showing that EBV-transformed lymphoblastoid cell lines established from the two CCD patients display the following features: (i) they have depleted thapsigargin-sensitive intracellular calcium stores; (ii) they exhibit release of calcium from intracellular stores in the absence of the addition of a pharmacological activator of the RYR1; and (iii) the unelicited calcium transient from the thapsigargin-sensitive stores could be blocked by dantrolene, a specific inhibitor of the skeletal muscle RYR (29,30). The 'unprompted' intracellular calcium transient was observed in 64% (9/14) of the experiments. In the remaining experiments we observed only the tail of the declining phase of the calcium transient. In this cell population as well, the size of the thapsigargin-sensitive stores was similar to that of the cells exhibiting a complete transient. The most likely explanation for the 'tail' of the transient, is that we did not capture the complete event of the 'unprompted' calcium transient but only its final part. The tail signal is reminiscent of that observed in fura-2 loaded cytotoxic T lymphocytes (32).

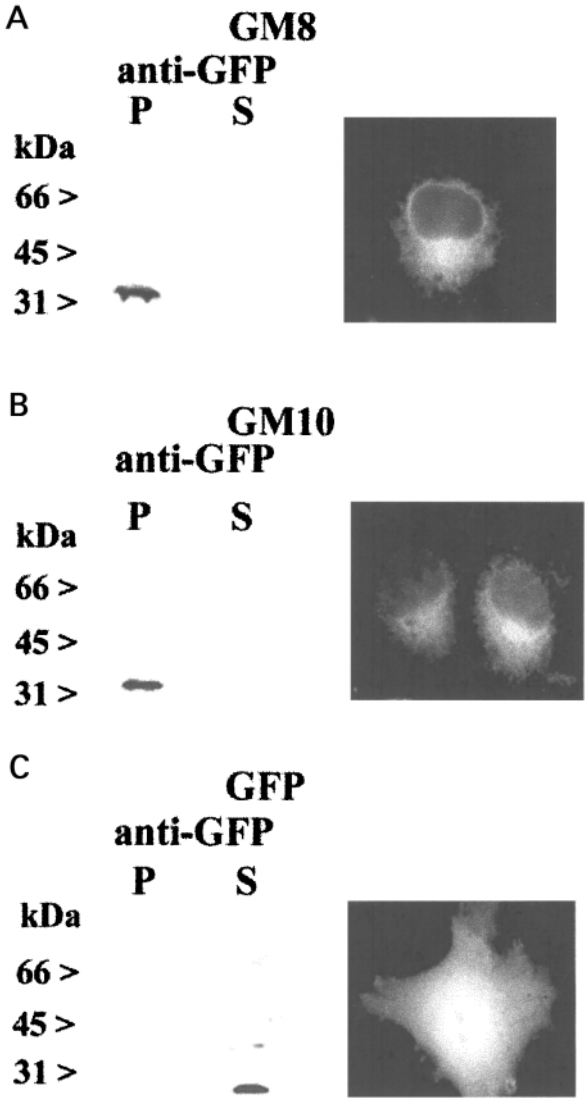

Figure 5. Fusion proteins encompassing amino acid residues V4830–4870 and 4907–4943 of the rabbit skeletal muscle RYR1 are integral membrane proteins. (**A** and **B**) Microsomes from Tsa201 cells transfected with the RYR1 cDNA constructs tagged with GFP were washed with high salt and 100 mM Na_2CO_3. Soluble proteins and proteins loosely associated with the membranes (S) were separated from integral membrane proteins (P) by differential centrifugation. (**C**) Tsa201 cells were transfected with pEGFP and proteins present in the microsomal or post microsomal soluble fraction were loaded on the PAG. Twenty micrograms of protein were loaded per lane, separated on a 10% SDS–PAGE, blotted onto nitrocellulose and probed with anti-GFP antibodies. The panels on the right show the GFP-fluorescence exhibited by COS-7 cells transfected with the plasmids (magnification ×1000).

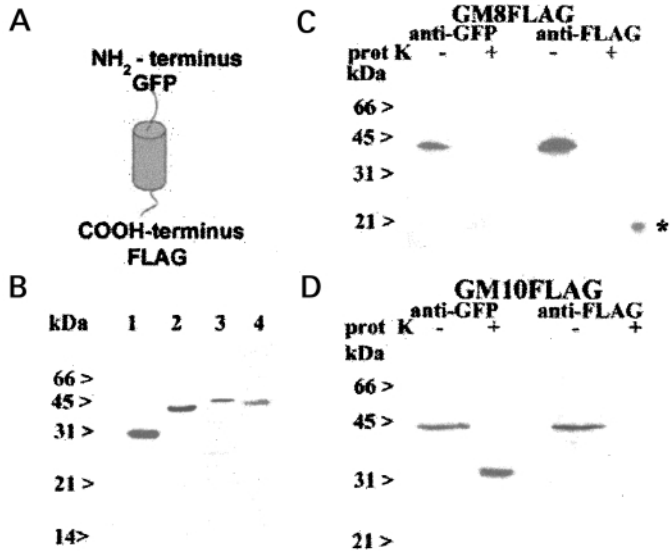

Figure 6. Membrane topology of fusion proteins GM8 and GM10. (**A**) Schematic representation of constructs used to transfect Tsa201 cells. A FLAG tag was added to the COOH-terminus of GM8 and GM10 as described in the Materials and Methods section. (**B**) The post microsomal supernatant of Tsa201 cells transfected with pEGFP and pEGFP-FLAG (lanes 1 and 2, respectively) or the microsomal fraction of Tsa201 cells transfected with GM8FLAG and GM10FLAG (lanes 3 and 4) were loaded on a 15% SDS–PAGE, blotted onto nitrocellulose, and probed with anti-GFP antibodies (20 µg protein/lane). (**C** and **D**) The microsomal fraction of Tsa201 cells transfected with GM8FLAG and GM10FLAG was treated with or without proteinase K; 10 µg protein were loaded per lane, separated on a 12.5% SDS–PAGE, blotted onto nitrocellulose and probed with anti-GFP or anti-FLAG antibodies. The asterisk indicates the immunoreactive band obtained after digestion of the GM8FLAG construct with proteinase K, when probed with anti-FLAG Abs.

We still do not know what causes the 'unprompted' calcium release in the EBV-immortalized lymphoblasts, but it appears to be an intrinsic characteristic of those cells carrying RYR mutations/deletions associated with CCD which affect the COOH-terminal amino acid sequences involved in the formation of the membrane spanning segments of the calcium release channel (24). In fact EBV-immortalized lymphoblasts from a patient carrying the recently identified CCD-linked RYR1 mutation P3527S (which should be located in the hydrophilic portion of the RYR, not adjacent to the pore forming region) (33), (i) did not show such 'unprompted' calcium release and (ii) had thapsigargin-sensitive intracellular calcium stores which were indistinguishable from those of controls (S. Treves, A. Ferreiro, N. Monnier and J. Lunardi, unpublished observations).

Interestingly, although the calcium release characteristics of the cell lines established from the daughter and her mother were similar, i.e. they had depleted thapsigargin-sensitive pools, there was a marked difference in the clinical severity between these two members of the family. This implies that *in vivo* other factors modulate the penetrance of the RYR deletion. Each individual may activate different compensatory mechanisms in muscle tissue and it seems that EBV-immortalized lymphocytes probably lack the proteins involved in these mechanisms. Alternatively, the phenotypic differences between mother and daughter may be linked to the levels of expression of RYR1 channels carrying the deletion *in vivo*, i.e. there may be differences in the number of homotetramers and heterotetramers carrying the RYR1 deletion. Clearly studies aimed at identifying the subunit composition of the channels *in vivo* are necessary to clarify this issue.

To determine the functional consequences of the deletion, cDNAs containing either wild-type or mutant cDNAs were transfected into HEK293 cells. The expressed proteins were characterized by [^{3}H]ryanodine binding and single channel

measurements. Both methods indicated a loss of regulation by Ca^{2+} and ryanodine, providing biochemical confirmation that the deletion is the likely cause of CCD. The mutant channels will require more detailed characterization, however we noted that the homozygous channels show constitutive K^+ and Ca^{2+} conductance, which may explain that the deletion in RYR1 influences the Ca^{2+} permeability. The mutant K^+ and Ca^{2+} conductances were lower than in wild-type, suggesting that the deleted amino acids lie close or may be a part of the pore-forming region of RYR1.

A great deal of information has been gathered on the nature and structure of the RYR domain involved in the formation of the conduction pore (34–36). Site-directed mutagenesis experiments and comparison of the sequence of the RYR with that of a potassium channel from *Streptomyces lividans*, whose crystal structure has been defined (37), have indicated that the amino acid residues lining the pore are defined by residues 4886–4910. The pore-forming domain overlaps with a region originally defined as M9 (3) and is adjacent to the region carrying the deletion, an area which is highly conserved in all vertebrate RYRs examined to date (cf. Fig. 2). The definition of the membrane topology of the latter region and that of the pore-forming domain is thus crucial to understand the exact role of RYR in the pathophysiology of CCD. Since the membrane topology of this area has not been fully elucidated, we designed a set of experiments to identify membrane spanning segments in this region of the RYR1. We provide experimental evidence that, when expressed as recombinant polypeptides in heterologous cells, domains M8 and M10 are indeed membrane spanning segments. The NH_2-terminus of M8 is cytoplasmic, while the region encompassing the deletion and connecting M8 to M10 is lumenal. On the other hand, the NH_2-terminus of M10 is in the lumen of the endoplasmic reticulum (see Fig. 7). The presence of the newly identified deletion causes a change in the charge of the segment directly adjacent to the pore: of the six deleted amino acids, two are positively (one arginine and one lysine) and one is negatively (glutamate) charged, resulting in an overall more negatively charged polypeptide. Studies aimed at determining the function of charged residues in segments adjacent to ion conducting pores have demonstrated that such changes in charge can greatly affect the conductance properties of the channel (37). In this case a reduced K^+ and Ca^{2+} conductance was recorded for the mutant channel.

In conclusion, in the present report we demonstrate that the functional characteristics of native and recombinant RYR1 carrying a seven amino acid deletion associated with CCD, are severely altered and that the deleted amino acids are part of a polypeptide segment connecting transmembrane segments M8 and M10 of the RYR1 calcium channel.

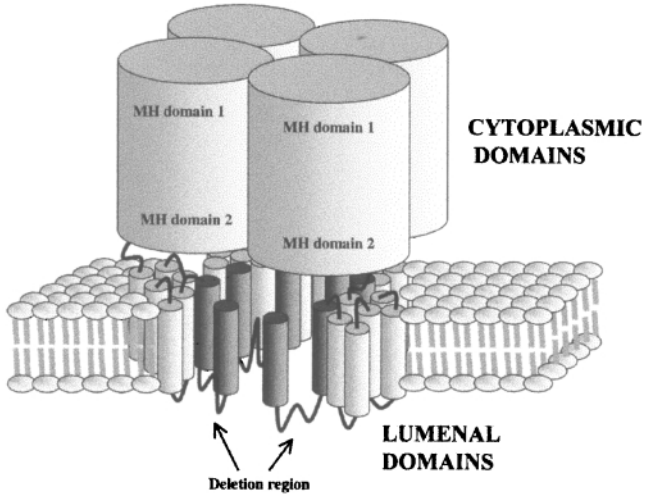

Figure 7. Cartoon depicting the proposed membrane topology of the COOH-terminal domain of RYR1. The functional calcium release channel is made up of four subunits. The putative regions involved in MH/CCD mutations are indicated as well as the location of the deletion studied in this paper. The dark grey cylinders in the bilayer represent transmembrane polypeptides GM8 and GM10 which were investigated in the present report.

MATERIALS AND METHODS

Patients' clinical details

The patient of Mediterranean origin was born by Caesarean section at term, after an uneventful pregnancy. At birth she had a left leg fracture and bilateral dislocation of hips that were treated conservatively (double nappies). Her motor development was delayed and she sat and crawled at 18 months. At 2 years she was reviewed at the Hammersmith Hospital and rehabilitated in calipers that she could use to stand with, but she could not walk unsupported. A muscle ultrasound showed a marked increase in echogeneicity and a needle muscle biopsy confirmed the diagnosis of CCD. Since then, the patient has been seen at yearly intervals. Now, at the age of 15 years she is able to walk unsupported in calipers but uses a wheel-chair for longer distances. Over time, she has developed a marked lumbar lordosis and a moderate thoracolumbar scoliosis which has been managed with a thoracolumbar orthosis. Overall, her mobility and strength have improved and she is attending regular school with good success. She occasionally complains of generalized muscle pain following prolonged walking.

Her mother was first seen at the Hammersmith Hospital at age of 31. Although she was asymptomatic, she was found to have some mild facial weakness, with inability to bury her eyelashes. A muscle ultrasound performed at the same time showed a marked increase in echogeneicity and a needle muscle biopsy showed a classical picture of CCD. Currently aged 43 she only complains of frequent muscle pain and cramps following even moderate exercise.

Lymphoblastoid cell lines

Mononuclear cells were isolated from peripheral blood leukocytes and transformed with EBV according to the protocol of Neitzel (38). Cells were cultured as described (26).

Mutation screening

Exons 98–103 of the RYR1 gene were screened for mutations by single-strand conformation analysis (SSCA) and direct sequencing as previously described (24). The presence of the RYR1 gene deletion in exon 101 was confirmed by PCR

amplification of genomic DNA as previously described (24). The presence of the deletion in the cDNA of EBV-immortalized lymphoblastoid cells was also verified by PCR as previously described (26). Briefly, poly(A^+) RNA was purified using a commercially available kit (Qiagen). mRNA was converted into cDNA using a cDNA synthesis kit, following the instructions provided by the manufacturer (Roche Applied Science). Amplification conditions were: 5 min at 95°C, followed by 40 cycles of 45 s annealing at 55°C, 45 s extension at 72°C, 30 s denaturation at 92°C and extension for 4 min at 72°C. The following forward and reverse primers spanning exons 100–101 were used to amplify the cDNA: 5′-TTC TTC TTT GCT GCC CAT CT and 5′-CGT CAT CAT GTC ATC ACA CTT C, respectively. The presence of the mutation was detected by electrophoresis in a 7.5% acrylamide gel and confirmed by sequencing.

Construction and expression of RYR1 deletion mutant

Deletion of nucleotides encoding amino acids 4862–4868 (corresponding to 4863–4869 of human RYR1) of rabbit RYR1 and insertion of three bases encoding tyrosine were performed by pfu polymerase-based chain reaction, using mutagenic oligonucleotides and the QuickChange site-directed mutagenesis kit (Stratagene, La Jolla, CA, USA) as described previously (34). Briefly, the COOH-terminal fragment (ClaI/XbaI, 14443/15276) of RYR1 cDNA was subcloned into the pBluescript vector and served as a template for PCR. The construct was confirmed by sequencing. The fragment with the deletion was cloned back into the original position of EcoRI/XbaI (11766/15276) fragment of RYR1. The full-length RYR1 cDNA with the deletion was constructed by ligating the three fragments (ClaI/XhoI, XhoI/EcoRI, EcoRI/XbaI with deletion) into the expression vector pCMV5 (ClaI/XbaI). Wild-type and mutant RYR1 cDNAs were transiently expressed in HEK293 cells transfected with Fugene 6 (Roche Applied Science), according to the manufacturer's instructions. Cells were maintained at 37°C and 5% CO_2 in high glucose Dulbecco's minimum essential medium containing 10% fetal bovine serum and plated the day before transfection. For each 10 cm tissue culture dish, 3–6 μg cDNA were used. Cells were harvested 42–48 h after transfection and crude membrane fractions were prepared as described (34).

[^{3}H]Ryanodine binding

B_{max} values of [^{3}H]ryanodine binding were determined by incubating crude membranes for 4 h at room temperature with a saturating concentration of [^{3}H]ryanodine (40 nM) in 20 mM imidazole, pH 7.0, 0.6 M KCl, 0.15 M sucrose, 20 μM leupeptin, 200 μM Pefabloc, and 100 μM Ca^{2+}. Non-specific binding was determined using 1000-fold excess of unlabelled ryanodine. After 4 h, aliquots of the samples were diluted with 8.5 vol of ice-cold water and placed on Whatman GF/B filters preincubated with 2% polyethyleneimine in water. Filters were washed with three 5 ml ice-cold 100 mM KCl, 1 mM KPipes, pH 7.0. The radioactivity remaining on the filters was determined by liquid scintillation counting to obtain bound [^{3}H]ryanodine.

Single channel recordings

Single channel measurements were performed by fusing crude microsomal fractions with Mueller–Rudin type bilayers containing phosphatidylethanolamine, phosphatidylserine, and phosphatidylcholine in the ratio 5:3:2 (25 mg total phospholipid/ml *n*-decane) (39). The side of the bilayer to which the membranes were added was defined as the *cis* (cytoplasmic) side. The *trans* (SR lumenal) side of the bilayer was defined as ground. Single channels were recorded in a symmetric KCl buffer solution (0.25 M KCl, 20 mM KHEPES, pH 7.4) containing the additions indicated in the text. Electrical signals were filtered at 2 kHz, digitized at 10 kHz and analysed using a commercially available software package (pClamp 8.2, Axon Instruments, Burlingame, CA, USA). P_o values in multichannel recordings were calculated using the formula $\Sigma\, iP_{o,i}/N$, where N is the total number of channels, and $P_{o,i}$ is channel open probability of the ith channel.

Construction and expression of putative RYR1 transmembrane segments M8–M10

The pEGFP-C1 plasmid (Clontech) was modified by introducing a tag similar to the 'FLAG' tag in the plasmid's multiple cloning site. To achieve this the oligodeoxynucleotide 5′-CGG GAT CCG GAA TTG CGA TCG GAC GAG CGA AAG ACT ACA AAG ACC ATG ACG GTG ATT ATA AAG ATC ATG ATA TCG ATT ACA AGG ATG ACG ATG ACA AGAC TAG TTC TAG AGC was used as a PCR template and amplified with the following forward and reverse primers: 5′-CGC GGA TCC GGA ATT and 5′-GGG GGG GGC TCT AGA, respectively. Amplification was performed as described above for mutation screening, using an annealing temperature of 51°C. The PCR amplified product was subcloned into the BamHI and Xba I sites of pEGFP-C1. The cDNAs encoding rabbit RYR1 putative transmembrane fragments M8 and M10 were amplified by PCR using the full-length RYR1 cDNA as template. Amplification was performed as described above using an annealing temperature of 54°C with the following forward and reverse primers: 5′-TCT GTC GAC CAC AAT GGG AAA and 5′-CCT CAT GTC GGA TCC GTC CTC, respectively and 60°C with the following forwards and reverse primers: 5′-CCC AGC GGT CGA CGA ATA CG and 5′-GCT CCT GCT GGG ATC GCA GCT. The SalI/BamHI restriction enzyme sequence was added to facilitate cloning and sequencing of the constructs. After digestion with the restriction enzymes SalI and BamHI, the PCR products were subcloned in frame into the pEGFP-C1 plasmid and into the modified pEGFP-C1 FLAG Tag plasmid. We thus obtained fusion proteins GM8 and GM8FLAG which encompass RYR1 residues V4830 to D4870 and fusion proteins GM10 and GM10FLAG which encompass RYR1 residues D4907 to L4943, respectively. All constructs were verified by direct sequencing. COS-7 cells were transfected using lipofectin and GFP-fluorescence was monitored as previously described (40). Tsa201 cells were grown at 37°C, 5% CO_2 in MEM (Gibco BRL) supplemented with Earl's salts, 10% fetal bovine serum and antibiotics. Cells were plated in 10 cm tissue culture dishes and transfected with 5–10 μg DNA per plate, using the $CaPO_4$ technique. Cells were harvested and subcellular fractions

prepared 48 h post transfection. Total microsomes were prepared from Tsa201 cells transfected with the EGFP, GM8, GM10, EGFP-FLAG, GM8FLAG and GM10FLAG cDNA constructs as previously described (26). A high-salt wash with 0.6 M KCl was added to remove proteins loosely associated with membranes. Integral membrane proteins were separated from their soluble counterpart by extraction with Na_2CO_3 as previously described (41). The pellets were resuspended in 0.25 M sucrose, 10 mM HEPES pH 7.4.

Proteinase K digestion

The microsomal pellets of Tsa201 cells transfected with the GM8FLAG and GM10FLAG were treated with proteinase K (Roche Applied Science) for 5 min at 27°C at different proteinase K/protein ratios (from 1/25 to 1/200) as previously described (41). The reaction was stopped by the addition of a cocktail of anti-protease inhibitors (Roche Applied Science) plus 1 mM PMSF and Laemmli loading buffer. Samples were placed at 95°C for 5 min and proteins were subsequently processed for SDS–PAGE. The intactness of the vesicles was checked by performing the tryptic digestion in the presence or absence of several detergents.

Electrophoresis and western blotting

Proteins were processed for SDS/PAGE, blotted onto nitrocellulose and probed with monoclonal anti-RYR1 (34), monoclonal anti-GFP (Roche Applied Science) and anti-FLAG tag (Sigma Chemicals, St Louis, MO, USA, Anti-Flag M2) antibodies. Peroxidase-conjugated anti-mouse IgG was used to detect the primary antibody followed by chemiluminescence.

Intracellular Ca^{2+} measurements

Changes in the intracellular calcium concentration of the lymphoblastoid cells were monitored with the fluorescent calcium indicator fura-2/AM (Sigma Chemicals, St Louis, MO, USA) as described (24,26,42). Fura-2 loaded cells (0.7×10^6/ml; final fura-2 concentration 5 μM) were resuspended in Ca^{2+}-free Krebs–Ringer medium containing 0.5 mM EGTA and placed in a cuvette thermostated at 37°C. Fluorescence changes (ratio 340/380 nm) were measured in an LS-50S Perkin–Elmer spectrofluorimeter equipped with a magnetic stirrer. All measurements were made in Ca^{2+}-free Krebs–Ringer buffer containing 0.5 mM EGTA. Experiments were performed at least four times on three different days.

Statistical analysis

For the two group comparisons, Student's *t*-test was used; the overall statistical significance level was set to 5%.

ACKNOWLEDGEMENTS

We greatly appreciate the co-operation of the CCD patients. We would like to thank Evgueni Voronkov and Daniel Pasek for expert technical assistance. This work was supported by grants from Telethon Italy (no. 1259), Ministero Universita' e Ricerca scientifica e Tecnologica 40%, ERBFMRXCT9600032 and HPRN-CT-2002-00331 from the European Union, United States Public Health grant AR18687 (to G.M.) and by the Departments of Anaesthesia, Kantonsspital Basel and Human Genetics, University of Wuerzburg. The Muscular Dystrophy Group grant to F.M. is also acknowledged.

REFERENCES

1. Sutko, J.L. and Airey, J.A. (1996) Ryanodine receptor Ca^{2+} release channels: does diversity in form equal diversity in function? *Physiol. Rev.*, **76**, 1027–1071.
2. Phillips, M.S., Fujii, J., Khanna, V.K., DeLeon, S., Yokobata, K., de Jong, P.J. and MacLennan, D.H. (1996) The structural organization of the human skeletal muscle ryanodine receptor (RYR1) gene. *Genomics*, **34**, 24–41.
3. Zorzato, F., Fujii, J., Otsu, K., Phillips, M., Green, N.M., Lai, F.A., Meissner, G. and MacLennan, D.H. (1990) Molecular cloning of cDNA encoding human and rabbit forms of the Ca^{2+} release channel (ryanodine receptor) of skeletal muscle sarcoplasmic reticulum. *J. Biol. Chem.*, **265**, 2244–2256.
4. Takeshima, H., Nishimura, S., Matsumoto, T., Ishida, H., Kangawa, K., Minamino, N., Matsuo, H., Ueda, M., Hanaoka, M., Hirose, T. *et al.* (1989) Primary structure and expression from complementary DNA of skeletal muscle ryanodine receptor. *Nature*, **339**, 439–445.
5. Brillantes, A.B., Ondrias, K., Scott, A., Kobrinsky, E., Ondriasova, E., Moschella, M.C., Jayaraman, T., Landers, M., Ehrlich, B.E. and Marks, A.R. (1994) Stabilization of calcium release channel (ryanodine receptor) function by FK506-binding protein. *Cell*, **77**, 513–523.
6. Marks, A.R., Marx, S.O. and Reiken S. (2002) Regulation of ryanodine receptors via macromolecular complexes. A novel role for leucine/isoleucine zippers. *Trends Cardiovasc. Med.*, **12**, 166–170.
7. Franzini-Armstrong, C. and Protasi, F. (1997) Ryanodine receptors of striated muscles: a complex channel capable of multiple interactions. *Physiol. Rev.*, **77**, 699–729.
8. Jurkat-Rott, K., McCarthy, T. and Lehmann-Horn, F. (2000) Genetics and pathogenesis of malignant hyperthermia. *Muscle Nerve*, **23**, 4–17.
9. McCarthy, T.V., Quane, K.A. and Lynch, P.J. (2000) Ryanodine receptor mutations in malignant hyperthermia and central core disease. *Hum. Mutat.*, **15**, 410–417.
10. Dirksen, R.T. and Avila, G. (2002) Altered ryanodine receptor function in central core disease: leaky or uncoupled Ca^{2+} release channels? *Trends. Cardiovasc. Med.*, **12**, 189–197.
11. Isaacs, H., Heffron, J.J. and Badenhorst, M. (1975) Central core disease. A correlated genetic, histochemical, ultramicroscopic, and biochemical study. *J. Neurol. Neurosurg. Psychiat.*, **38**, 1177–1186.
12. Shy, G.M. and Magee, K.R. (1956) A new congenital non-progressive myopathy. *Brain*, **79**, 160.
13. Shuaib, A., Paasuke, R.T. and Brownell, K.W. (1987) Central core disease. Clinical features in 13 patients. *Medicine (Baltimore)*, **66**, 389–396.
14. Hayashi, K., Miller, R.G. and Brownell, A.K. (1989) Central core disease: ultrastructure of the sarcoplasmic reticulum and T-tubules. *Muscle Nerve*, **12**, 95–102.
15. Greenfield, J.G., Cornman, T. and Shy, G.M. (1958) The prognostic value of the muscle biopsy in the "floppy infant". *Brain*, **81**, 461.
16. Gronert, G., Antonigni, J. and Pessah, I. (2000) *Malignant Hyperthermia*, 5th edn, Anesthesia, Miller, R. (ed.). Churchill Livingstone, New York.
17. Denborough, M.A. and Lovell, R.R.H. (1960) Anaesthetic deaths in a family. *Lancet*, **2**, 45.
18. Denborough, M. (1998) Malignant hyperthermia. *Lancet*, **352**, 1131–1136.
19. Larach, M.G., Localio, A.R., Allen, G.C., Denborough, M.A., Ellis, F.R., Gronert, G.A., Kaplan, R.F., Muldoon, S.M., Nelson, T.E., Ording, H. *et al.* (1994) A clinical grading scale to predict malignant hyperthermia susceptibility. *Anesthesiology*, **80**, 771–779.
20. MacLennan, D.H. and Phillips, M.S. (1992) Malignant hyperthermia. *Science*, **256**, 789–794.
21. Wappler, F., Fiege, M., Steinfath, M., Agarwal, K., Scholz, J., Singh, S., Matschke, J. and Schulte Am Esch, J. (2001) Evidence for susceptibility to malignant hyperthermia in patients with exercise-induced rhabdomyolysis. *Anesthesiology*, **94**, 95–100.
22. Wingard, D.W. (1974) Letter: Malignant hyperthermia: a human stress syndrome? *Lancet*, **2**, 1450–1451.

23. Monnier, N., Romero, N.B., Lerale, J., Landrieu, P., Nivoche, Y., Fardeau, M. and Lunardi, J. (2001) Familial and sporadic forms of central core disease are associated with mutations in the C-terminal domain of the skeletal muscle ryanodine receptor. *Hum. Mol. Genet.*, **10**, 2581–2592.
24. Tilgen, N., Zorzato, F., Halliger-Keller, B., Muntoni, F., Sewry, C., Palmucci, L.M., Schneider, C., Hauser, E., Lehmann-Horn, F., Muller, C.R. and Treves, S. (2001) Identification of four novel mutations in the C-terminal membrane spanning domain of the ryanodine receptor 1: association with central core disease and alteration of calcium homeostasis. *Hum. Mol. Genet.*, **10**, 2879–2887.
25. Lynch, P.J., Tong, J., Lehane, M., Mallet, A., Giblin, L., Heffron, J.J., Vaughan, P., Zafra, G., MacLennan, D.H. and McCarthy, T.V. (1999) A mutation in the transmembrane/luminal domain of the ryanodine receptor is associated with abnormal Ca^{2+} release channel function and severe central core disease. *Proc. Natl Acad. Sci. USA*, **96**, 4164–4169.
26. Girard, T., Cavagna, D., Padovan, E., Spagnoli, G., Urwyler, A., Zorzato, F. and Treves, S. (2001) B-lymphocytes from malignant hyperthermia-susceptible patients have an increased sensitivity to skeletal muscle ryanodine receptor activators. *J. Biol. Chem.*, **276**, 48077–48082.
27. Sei, Y., Gallagher, K.L. and Basile, A.S. (1999) Skeletal muscle type ryanodine receptor is involved in calcium signaling in human B lymphocytes. *J. Biol. Chem.*, **274**, 5995–6002.
28. O'Connell, P.J., Klyachko, V.A. and Ahern, G.P. (2002) Identification of functional type 1 ryanodine receptors in mouse dendritic cells. *FEBS Lett.***512**, 67–70.
29. Paul-Pletzer, K., Palnitkar, S.S., Jimenez, L.S., Morimoto, H. and Parness, J. (2001) The skeletal muscle ryanodine receptor identified as a molecular target of [^{3}H]azidodantrolene by photoaffinity labeling. *Biochemistry*, **40**, 531–542.
30. Zhao, F., Li, P., Chen, S.R., Louis, C.F. and Fruen, B.R. (2001) Dantrolene inhibition of ryanodine receptor Ca^{2+} release channels. Molecular mechanism and isoform selectivity. *J. Biol. Chem.*, **276**, 13810–13816.
31. Xu, L., Tripathy, A., Pasek, D.A. and Meissner, G. (1999) Ruthenium red modifies the cardiac and skeletal muscle Ca^{2+} release channels (ryanodine receptors) by multiple mechanisms. *J. Biol. Chem.*, **274**, 32680–32691.
32. Treves, S., Di Virgilio, F., Cerundolo, V., Zanovello, P., Collavo, D. and Pozzan, T. (1987) Calcium and inositolphosphates in the activation of T cell-mediated cytotoxicity. *J. Exp. Med.*, **166**, 33–42.
33. Ferreiro, A., Monnier, N., Romero, N.B., Leroy, J.P., Bönnemann, C., Haenggeli, C.A., Straub, V., Voss, W.D., Nivoche, Y., Jungbluth, H. *et al.* (2002) A recessive form of Central Core Disease, transiently presenting as Multi-Minicore Disease, is associated with a homozygous mutation in the ryanodine receptor type 1 gene. *Ann. Neurol.*, **51**, 750–759.
34. Gao, L., Balshaw, D., Xu, L., Tripathy, A., Xin, C. and Meissner, G. (2000) Evidence for a role of the lumenal M3-M4 loop in skeletal muscle Ca^{2+} release channel (ryanodine receptor) activity and conductance. *Biophys. J.*, **79**, 828–840.
35. Du, G.G., Guo, X., Khanna, V.K. and MacLennan, D.H. (2001) Functional characterization of mutants in the predicted pore region of the rabbit cardiac muscle Ca^{2+} release channel (ryanodine receptor isoform 2). *J. Biol. Chem.*, **276**, 31760–31771.
36. Chen, S.R., Li, P., Zhao, M., Li, X. and Zhang, L. (2002) Role of the proposed pore-forming segment of the Ca^{2+} release channel (ryanodine receptor) in ryanodine interaction. *Biophys. J.*, **82**, 2436–2447.
37. Doyle, D.A., Morais Cabral, J., Pfuetzner, R.A., Kuo, A., Gulbis, J.M., Cohen, S.L., Chait, B.T. and MacKinnon, R. (1998) The structure of the potassium channel: molecular basis of K^+ conduction and selectivity. *Science*, **280**, 69–77.
38. Neitzel, H. (1986) A routine method for the establishment of permanent growing lymphoblastoid cell lines. *Hum. Genet.*, **73**, 320–326.
39. Tripathy, A., Xu, L., Mann, G. and Meissner, G. (1995) Calmodulin activation and inhibition of skeletal muscle Ca^{2+} release channel (ryanodine receptor). *Biophys. J.*, **69**, 106–119.
40. Treves, S., Pouliquin, P., Moccagatta, L. and Zorzato, F. (2002) Functional properties of EGFP-tagged skeletal muscle calcium-release channel (ryanodine receptor) expressed in COS-7 cells: sensitivity to caffeine and 4-chloro-m-cresol. *Cell Calcium*, **31**, 1–12.
41. Zorzato, F., Anderson, A.A., Ohlendieck, K., Froemming, G., Guerrini, R. and Treves, S. (2000) Identification of a novel 45 kDa protein (JP-45) from rabbit sarcoplasmic-reticulum junctional-face membrane. *Biochem. J.*, **351**, 537–543.
42. Grynkiewicz, G., Poenie, M. and Tsien, R.Y. (1985) A new generation of Ca^{2+} indicators with greatly improved fluorescence properties. *J. Biol. Chem.*, **260**, 3440–3450.